Canadian Chemical Transactions Year 2016 | Volume 4 | Issue 1 | Page 99-120

*Research Article*

DOI:10.13179/canchemtrans.2016.04.01.0268

# Molecular Investigation and Characterization of 5-(3-bromo-4-fluorobenzylidene)pyrimidine-2,4,6(1H,3H,5H)-trione: A Molecular Orbital Approach

**D. Durgadevi[1], A. Dhandapani[1], S. Manivarman[1]*, S. Subashchandrabose[2*]**

*[1]PG and Research department of chemistry, Government Arts College, C-Mutlur, Chidambaram-608102, Tamil Nadu, India.*
*[2]Centre for Research & Development, PRIST University, Vallam, Thanjavur-613403, Tamil Nadu, India.*

**Corresponding Author, Email: drsmgac@gmail.com (S. M); sscbphysics@gmail.com (S. S.)*

***Received:*** *December 21, 2015* ***Revised:*** *February 1, 2016* ***Accepted:*** *February 2, 2016* ***Published:*** *February 8, 2016*

**Abstract:** 5-(3-Bromo-4-Fluorobenzylidine)pyrimidine-2,4,6(1H,3H,5H)-trione(BFPT) was synthesized and investigated by experimental and theoretical methodologies. The spectral characterization was made using FT-IR, FT-Raman and density functional calculation with B3LYP/6-31G(d,p) level of theory. The optimization of predicted molecule has been studied using the same level of basis set. To study the vibrational behaviour, the FT-IR and FT-Raman spectra were recorded in the region between 400-4000 $cm^{-1}$ and 50-4000 $cm^{-1}$ respectively. Both experimental and theoretical results were compared and analysed the characteristics of the title compound. Non-linear optical activity was investigated and found that BFPT compound is a good non-linear material. The natural bond orbital analysis, molecular electrostatic potential and band gap energies were analysed and the reactive path of the BFPT molecule were also studied.

**Keywords:** Molecular Orbital; Density Functional Theory; FT-IR; Raman; Non-linear Optical Activity

## 1. INTRODUCTION

Barbituric acid is an important compound with a heterocyclic structure and possibility of existing in several tautomeric forms because of mobility of the hydrogen atoms in its molecules. Some experimental investigations of barbituric acid and its derivatives mainly tuned to its application in medicine and as dye in chemical industry [1,2]. Barbituric acid derivatives possess a rather broad spectrum of therapeutic activity. Substituted heterocyclic/substituted aryl systematic variation at the $5^{th}$-position of barbituric [3-5] or thiobarbituric [6-8] acids nucleus remarkably increases the antiepileptic activity. In particular, pyrimidine-derived biomolecules have received much attention from spectroscopists, drug, clinical and industrial researchers because of their therapeutic importance [9–17]. Barbiturates are a class of central nervous system depressants [18] utilized as sedatives, sleeping agents,

hypnotics, anxiolytics, anticonvulsants, and anaesthetics [19]. In addition, they have additional pharmacological activities as antioxidant anxiolitics, analeptics, anti-AIDA, immune modulator, anticancer agents and in other psychiatric disorders and possess effects on motor and sensory functions [20–25]. New pharmacological properties of barbituric acid derivatives established in recent years significantly expanded the application range of barbiturates [26].

The biological significance of the pyrimidine derivatives has promoted us to synthesize a new substituted barbituric acid and to evaluate them for their anti-microbial activity. In this present investigation, a new pyrimidine derivative was synthesized by condensation of 3-bromo-4-fluourobenzaldehyde with barbituric acid. Attention has been focused on structural activity relationship. Vibrational analysis by Density Functional Theory (DFT) approaches are the powerful tool for the determination of various molecular properties and molecular geometry of the molecule. Thermodynamic data such as enthalpy of formation are often helpful in the understanding of the structural conformational and reactivity trends exhibited by molecules. The data are needed to estimate the amount of energy released or adsorbed in a chemical reaction, in calculating other thermodynamics functions, and more importantly in assessing the relative stability of molecules. One of the purposes of thermochemistry is to derive the enthalpy of formation of compound from their elements and to relate the energy to structure and chemical binding [27].

The main objective of this investigation is to calculate the molecular geometry and energy of the title compound by DFT method by using B3LYP/6-31G(d,p) level of theory. However, literature survey reveals that to the best of our knowledge, the quantum chemical calculations for BFPT have not been reported so far. Therefore, the present investigation using DFT method of calculations along with experimental characterization of FT-IR, FT-Raman spectra were undertaken to study the vibrational spectra and various normal modes with greater wavenumber accuracy. HOMO-LUMO analysis have been carried out to elucidate the information regarding energy gap and charge transfer within the molecule, also its NLO property, molecular electrostatic potential (MEP) and thermodynamic property of the title compound.

## 2. COMPUTATIONAL AND EXPERIMENTAL METHODS

*Computational Details*

Gaussian 03 quantum chemical software was used in all calculations. Optimized structural parameters and vibrational wavenumbers for the BFPT molecule were calculated by using B3LYP functional with 6-31G(d,p) basis set. The vibrational modes were assigned on the basis of PED analysis using VEDA4 program [28]. The calculated harmonic vibrational wavenumbers were scaled down uniformly by a factor of 0.9608 for B3LYP/6-31G(d,p) level of theory, which accounts for systematic errors caused by basis set incompleteness, neglect of electron correlation and vibrational anhormonicity [29,30].

*Experimental*

*Synthesis of barbituric acid (Stage-I)*

In a round-bottomed flask fitted with a reflux condenser, 2.3 g (0.1 mol) of finely cut sodium is dissolved in 50 ml of absolute alcohol. To this solution 16.01g (0.1 mol) of ethyl malonate followed by 6.006g (0.1mol) of dry urea dissolved in 50 ml of hot (70°) absolute alcohol are added. After being well shaken the mixture is refluxed for seven hours on an oil bath heated to 110°C. A white solid separates rapidly. After the reaction is completed100 ml of hot (50°) water is added and then enough hydrochloric acid to make the solution acidic. The resulting clear solution is filtered and cooled in an ice bath overnight. The white product is collected on a Buchner funnel, washed with 50 cc. of cold water and then dried in an oven at 105-110°C for three to four hours and recrystallized from ethanol. The yield of barbituric acid is 75%.

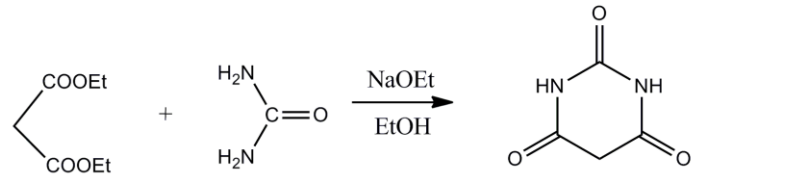


Diethylmalonate Urea Pyrimidine-2,4,6(1H,3H,5H)-trione

(Barbituric acid)

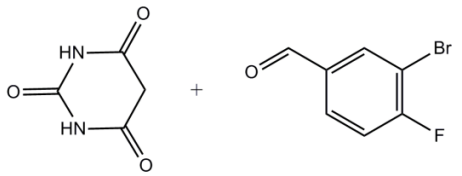


Barbituric acid 3-Bromo-4-Fluoro benzaldehyde

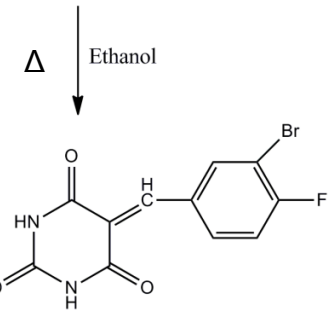


5-(3-bromo-4-fluorobenzylidene)pyrimidine-2,4,6(1*H*,3*H*,5*H*)-trione

## 3. RESULTS AND DISCUSSION

### *3.1 Structural determination by NMR spectra*

*5-(3-bromo-4-fluorobenzylidene)pyrimidine-2,4,6(1H,3H,5H)-trione:*

$^{1}$H-NMR (400 MHz, DMSO$d_6$): δ = 7.48-7.44 (m, 1H), 7.98-7.95 (m,1H), 8.15-8.13 (m,1H), 9.0 (s,1H, =CH).;$^{13}$C-NMR (100 MHz, DMSO$d_6$): δ= 109.5, 116.7, 117.47, 126.78, 131.5, 136.1, 161.4, 163.9, 170.2.; IR (KBr) νcm$^{-1}$, 3444, 3221 (NH), 3115 (Aromatic C–H), 1691 (C=O), 1593 (C=C).

The newly synthesized compound BFPT was confirmed by FT-IR and NMR spectral analysis. The appearance of totally four signals in the $^{1}$H-NMR and ten signals in $^{13}$C-NMR spectrum confirm the formation of required product. The observed $^{1}$H-NMR signal at 7.4, 7.9 and 8.1ppm are corresponding to the three aromatic protons which evident that the compound containing only one aromatic ring. The strong peaks observed at 1691 cm$^{-1}$ in FT-IR and the characteristic peak at 163 and 161 ppm in $^{13}$C NMR is clearly indicates the presence of carbonyl groups in this compound. Further, the FT-IR signal at 1593 cm$^{-1}$ confirms C=C linkage.

*3.2 Molecular investigation of 5-(3-bromo-4-fluorobenzylidene)pyrimidine-2,4,6(1H,3H,5H)-trione*

*3.2.1 Molecular geometry*

The optimized molecular structure along with the numbering scheme for BFPT is shown in Fig.1. The optimized geometrical parameters are calculated using B3LYP/6-31G(d,p) level of theory and also listed in the Table1. There is no exact crystal data available for this compound. Hence, the optimized geometrical parameters are compared with available crystal data of analogous molecule from the literature.

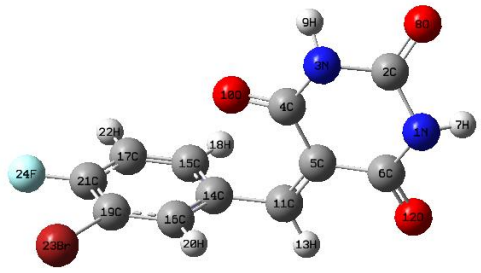


**Figure 1.** Optimized structure of BFPT.

The bond length of phenyl ring $C_{14}$–$C_{11}$, $C_{14}$–$C_{15}$, $C_{16}$–$C_{19}$ and $C_{17}$–$C_{21}$ are 1.452, 1.413, 1.385 and 1.319 Å respectively. In which the bond length of $C_{16}$–$C_{19}$ and $C_{17}$–$C_{21}$ are slightly lower due to the presence of electronegative atoms. The bond distance of C=C lies in the range of 1.368-1.416 Å and the bond length for $C_2$–$N_1$, $C_6$–$N_1$, $C_2$–$N_3$ and $C_4$–$N_3$ are calculated about 1.386, 1.390, 1.387 and 1.394 Å, respectively. These values are in agreement with X–ray diffraction data [31]. Similarly C=C and C=O groups bond length are calculated about 1.01 and 1.22 Å at B3LYP/6-31G(d,p) respectively, which also shows satisfactory agreement with the above crystal data.

In our study, the C–N–C angle in pyrimidine ring differs nearly by 1º and their magnitude found to be similar to the crystal data [33]. The bond angle of $C_5$–$C_4$–$N_3$ and $C_5$–$C_6$–$N_1$ are 115.33 and 116.05º respectively. The four outer angles of pyrimidine ring $C_2$–$N_1$–$H_7$, $C_6$–$N_1$–$H_7$, $C_2$–$N_3$–$H_9$, $C_4$–$N_3$–$H_9$ are found to almost same for uracil [32]. The angle of $C_4$–$C_5$–$C_6$ in pyrimidine ring is 118.62º, also $C_7$–$C_8$–$O_7$ and $C_7$–$C_{10}$–$O_5$ angles are 124.34 and 126.52º respectively. These bond angles are in agreement with literature [33].

The bond angles $C_6$–$C_5$–$C_{11}$, $C_{11}$–$C_5$–$C_4$ and $C_4$–$C_5$–$C_6$ in the centre of $C_5$ atom and their bond angles are 113.48, 127.89 and 118.62º respectively. The sum of these angles 359.99 indicating that the $C_5$ atom is of $sp^2$ hybridization type. In addition, the bond angles $C_5$–$C_{11}$–$H_{13}$, $C_{14}$–$C_{11}$–$H_{13}$ and $C_5$–$C_{11}$–$C_{14}$ in the centre of $C_{11}$ are 109.97, 112.10 and 137.91º. The total sum to 359.98º which shows that $C_{11}$ atom is also of $sp^2$ hybridization. So the title compound has good conjugation. The bond angles of C–C–C in phenyl ring lies in the range of 118–120º signifying all the carbon atoms are $sp^2$ hybridized which are in agreement with the literature value [34].

**Table 1.** Bond parameters of BFPT

| Bond length | (Å) | Bond angle | ( º) | Bond angle | ( º) |
|---|---|---|---|---|---|
| $C_{11}$-$H_{13}$ | 1.089 | $C_5$-$C_{11}$-$H_{13}$ | 109.979 | $C_{14}$-$C_{15}$-$C_{17}$ | 120.429 |
| $C_{15}$-$H_{18}$ | 1.080 | $H_{13}$-$C_{11}$-$C_{14}$ | 112.10 | $C_{17}$-$C_{15}$-$H_{18}$ | 120.472 |
| $C_{16}$-$H_{20}$ | 1.084 | $N_1$-$C_2$-$N_3$ | 113.5273 | $C_{15}$-$C_{17}$-$C_{21}$ | 120.078 |
| $C_{17}$-$H_{22}$ | 1.084 | $C_6$-$C_5$-$C_{11}$ | 113.484 | $C_{17}$-$C_{21}$-$C_{19}$ | 120.942 |
| $C_4$-$C_5$ | 1.479 | $C_{11}$-$C_{14}$-$C_{16}$ | 114.707 | $C_{14}$-$C_{16}$-$C_{19}$ | 121.381 |
| $C_5$-$C_6$ | 1.500 | $C_2$-$N_1$-$H_7$ | 115.960 | $C_{15}$-$C_{17}$-$H_{22}$ | 121.312 |
| $C_{11}$-$C_{14}$ | 1.452 | $C_2$-$N_3$-$H_9$ | 115.558 | $C_{16}$-$C_{19}$-$Br_{23}$ | 121.178 |
| $C_{14}$-$C_{15}$ | 1.413 | $C_4$-$N_3$-$H_9$ | 115.673 | $N_1$-$C_2$-$O_8$ | 123.373 |
| $C_{16}$-$C_{19}$ | 1.385 | $N_3$-$C_4$-$C_5$ | 115.336 | $N_3$-$C_2$-$O_8$ | 123.098 |
| $N_1$-$C_2$ | 1.38 | $C_6$-$N_1$-$H_7$ | 116.347 | $C_5$-$C_6$-$O_{12}$ | 124.345 |
| $N_1$-$C_6$ | 1.390 | $N_1$-$C_6$-$C_5$ | 116.055 | $C_5$-$C_4$-$O_{10}$ | 126.524 |
| $N_3$-$C_4$ | 1.394 | $N_3$-$C_4$-$O_{10}$ | 118.139 | $C_{11}$-$C_{14}$-$C_{15}$ | 127.169 |
| $C_4$-$O_{10}$ | 1.224 | $C_4$-$C_5$-$C_6$ | 118.620 | $C_2$-$N_1$-$C_6$ | 127.692 |
| $C_6$-$O_{12}$ | 1.221 | $C_{15}$-$C_{14}$-$C_{16}$ | 118.123 | $C_4$-$C_5$-$C_{11}$ | 127.895 |
| $C_5$-$C_{11}$ | 1.368 | $C_{19}$-$C_{16}$-$H_{20}$ | 118.794 | $C_2$-$N_3$-$C_4$ | 128.768 |
| $C_{14}$-$C_{16}$ | 1.416 | $C_{21}$-$C_{17}$-$H_{22}$ | 118.609 | $C_5$-$C_{11}$-$C_{14}$ | 137.919 |
| $C_{15}$-$C_{17}$ | 1.388 | $N_1$-$C_6$-$O_{12}$ | 119.599 | $C_{21}$-$C_{19}$-$Br_{23}$ | 119.776 |
| $C_{19}$-$C_{21}$ | 1.396 | $C_{14}$-$C_{15}$-$H_{18}$ | 119.097 | $C_{17}$-$C_{21}$-$F_{24}$ | 119.243 |
| $C_{19}$-$Br_{23}$ | 1.897 | $C_{14}$-$C_{16}$-$H_{20}$ | 119.824 | $C_{19}$-$C_{21}$-$F_{24}$ | 119.814 |

3.2.2 Vibrational assignment

The molecule BFPT contains phenyl ring, carbonyl groups and halogens. It consists 24 atoms, hence can have 66 normal modes of vibrations. The harmonic wavenumber calculations were performed with B3LYP/6-31G(d,p) level of theory. The title molecule belongs to $C_1$ point group symmetry. The

recorded FT-IR, FT-Raman, calculated wavenumbers, intensities, force constant and reduced masses are given in Table S1. The comparison of experimental and theoretical vibrational spectra of BFPT is shown in Figs. 2 & 3. The potential energy distributions for all fundamental vibrations were calculated using VEDA4 program.

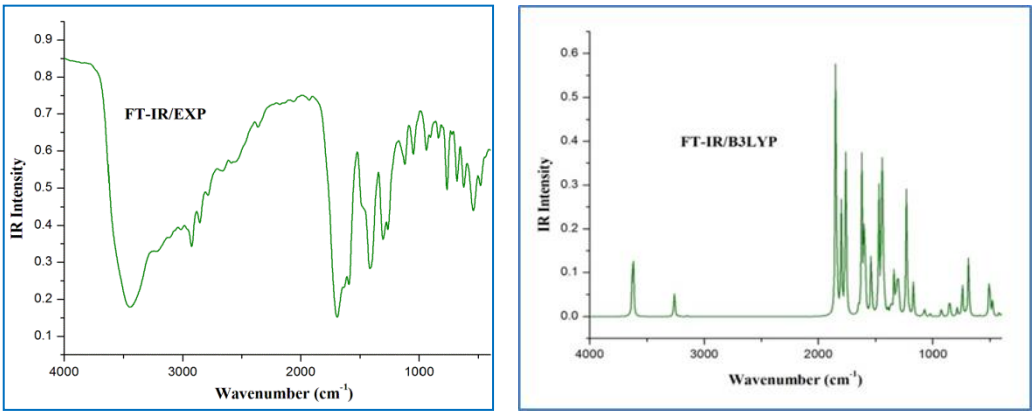


**Figure 2.** The recorded and theoretical FT-IR spectra of BFPT

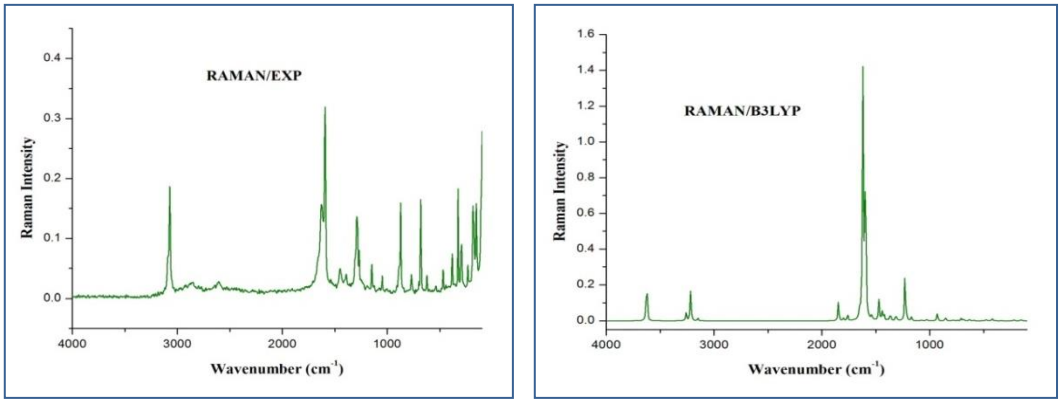


**Figure 3.** The recorded and theoretical FT-Raman spectra of BFPT

*3.2.2.1 C-H vibrations*

Aromatic compounds commonly exhibit multiple weak bands in the region 3100-3000 $cm^{-1}$[35,36] due to aromatic C−H stretching vibration. Accordingly, in the present study the C–H vibrations of the BFPT molecule are observed at 3115$cm^{-1}$ in the FT-IR and 3074 $cm^{-1}$ in FT-Raman spectrum are in good agreement with theoretical wavenumbers at 3133 $cm^{-1}$and 3088 $cm^{-1}$ respectively. The aromatic C-H in-plane-bending and out-of-plane bending vibrations observed at 1300-1000 $cm^{-1}$ and 900-690 $cm^{-1}$ respectively [37, 38]. The peak observed at 1120 $cm^{-1}$ in FT-IR spectrum is assigned for C–H in-plane-bending vibration. The infrared band observed at 941 $cm^{-1}$ is assigned to C–H out-of-plane bending vibration which is coincide with calculated value found at 967 $cm^{-1}$.

It is well known that the aliphatic C−H stretching vibrations are observed at lower wavenumber than the ring C−H stretching vibrations. The $C_{11}$−$H_{13}$ stretching vibration has been observed at 3012 $cm^{-1}$ in FT-IR and is lesser than the aromatic C−H stretching vibrations and this value has good agreement with theoretical wavenumber at 3027 $cm^{-1}$.

*3.2.2.2 Ring Vibrations*

The aromatic ring carbon–carbon stretching vibrations occur in the region 1650-1430 $cm^{-1}$[39]. The actual position of these modes are determined not so much by the nature of the substituents but by the form of substitution around the ring [40], although heavy halogens cause the frequency to diminish undoubtedly [41]. As predicted in the earlier reference, in the present work the strong C=C aromatic stretching is observed at 1593 $cm^{-1}$ in FT-IR and 1593$cm^{-1}$, 1538 $cm^{-1}$ in FT-Raman spectrum, respectively. These values show well agreement with calculated values at 1584 $cm^{-1}$ and 1533 $cm^{-1}$. The linkage formed between pyrimidine ring and phenyl ring at the position of $C_{11}$–$C_5$ observed at 1413 $cm^{-1}$ and it show good accordance with calculated value at 1413 $cm^{-1}$ and also in consistent with literature values [42].

The C–C stretching in phenyl ring is calculated at 1311 and 1364 $cm^{-1}$. These vibrations are in line with experimental value at 1303 $cm^{-1}$ in FT-IR spectrum. The stretching vibration of $C_6$–$C_5$ bond in pyrimidine ring observed at 1049 and 1047 $cm^{-1}$ in FT-IR and FT-Raman spectra. These values show good agreement with the calculated wavenumber at 1041 $cm^{-1}$.

*3.2.2.3 C=O vibrations*

The carbonyl C=O stretching vibration is expected to occur in the region 1715-1680 $cm^{-1}$[43, 44]. In the present investigation, carbonyl vibrations observed at 1691 $cm^{-1}$ in FT-IR spectrum and this wavenumber coincides well with theoretically calculated wavenumber at 1692 $cm^{-1}$ in B3LYP method and also find support from the literature [45]. Furthermore, the observed bands at 765$cm^{-1}$(FT-IR) and 769 $cm^{-1}$(FT-Raman) have been assigned to the C=O out-of-plane bending vibrations. Similar vibration has been observed at721$cm^{-1}$(FT–IR)/721$cm^{-1}$(FT–Raman) for C=O out-of-plane bending vibration of tetrahydropyrimidine [46].

*3.2.2.5 C–X Vibrations*

The bromo and fluoro substituted aromatic compounds absorbs strongly in the region of 690-515 $cm^{-1}$ and 1250-1120 $cm^{-1}$ respectively for stretching vibrations. The C–Br stretching vibration is assigned at 682 and 683 $cm^{-1}$ in FT-IR and FT-Raman respectively. This value consistent with computed value (681$cm^{-1}$) at mode no. 40 and supported by the literature at 656 $cm^{-1}$[50]. A weak band at 1263 $cm^{-1}$in FT-IR and 1267 $cm^{-1}$ in FT-Raman spectra are due to the strong coupling between stretching vibrations of fluorine and skeletal vibrations. These values are coinciding with calculated wavenumber at 1262 $cm^{-1}$.

*3.3 Molecular electrostatic potential*

Molecular electrostatic potential (MEP) represents a point in the space around the molecule to provide an indication of net electrostatic effect produced at that point by total charge distribution

(electron + nuclei) of the molecule and correlated with dipole moments, chemical reactivity, electronegativity, partial charges [51]. The importance of MEP lies in the fact that it simultaneously displays molecular size, shape as well as positive, negative and neutral electrostatic potential region in terms of colour grading also very useful in research of molecular structure with its physiochemical property.

The different values of the electrostatic potential on the surface of the molecule are represented by different colours. The red colour represents most negative electrostatic potential (electrophilic region) and the positive region which preferred site for nucleophilic attack symptoms as blue colour and green represents regions close to zero potential or neutral site [52,53]. The red region refers to the areas which favour interaction between lone pair oxygen and adjacent hydrogen atom. The MEP of BFPT shown in Fig. 4. The negative potential shows the acceptor nature refers to carbonyl groups of pyrimidine ring. Whereas the positive potential or donor nature is around N–H group of pyrimidine ring and the neutral region (green colour) refers to phenyl ring.

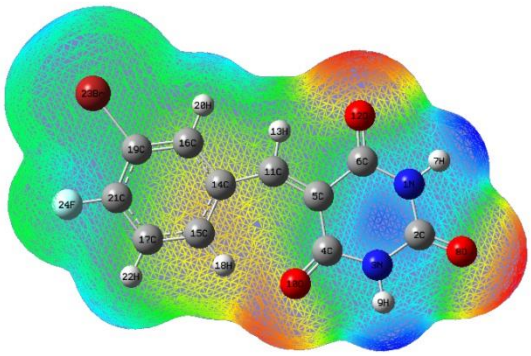

**Figure 4.** Molecular electrostatic potential map of BFPT.

*3.4 Mulliken population analysis*

The calculation of atomic charges has an important role in the application of quantum chemical calculation to molecular system [54]. Because, the atomic charges affect many properties such as dipole moment, electronic structure and polarizability [55]. The atomic charge of individual atom and its total value of the investigated compound have been obtained by mulliken population analysis are depicted in Table S2 and the graphical plot shown in Fig. 5. From the table S2, we can observe that the atomic charge of the BFPT molecule in the range from –0.609 to 0.603. The highest positive value 0.745 is exhibited by $C_2$ atom while the negative value –0.609 is exhibited by $N_1$ atom. It could be observed that entire oxygen atom possessed the negative value.

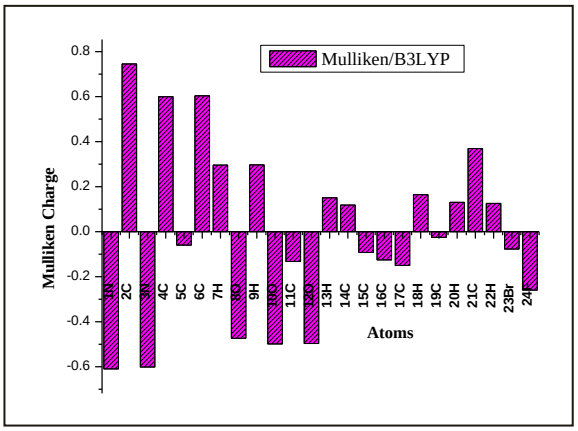


**Figure 5.** Mulliken atomic charges of BFPT

*3.5 Frontier molecular orbital analysis*

The π electron cloud moment from donor to acceptor can make the molecule highly polarized through the single-double path when it changes from the ground state to the excited state. Both the highest occupied molecular orbital (HOMO) and the lowest unoccupied molecular orbital (LUMO) are the main orbitals taking part in chemical stability. The HOMO represents the ability to donate an electron, LUMO as an electron acceptor represents the ability to obtain an electron [56]. The LUMO and HOMO energies have been calculated by B3LYP/6-31G(d,p) level of theory (Fig. 6).

Considering the chemical hardness, large HOMO-LUMO gap means a hard molecule and small HOMO-LUMO gap means a soft molecule. One can also relate the stability of the molecule to hardness, which means that molecule with least HOMO-LUMO gap means it is more reactive and the soft molecules are more polarizable than the hard ones because they need small energy to excitation [57]. The frontier molecules orbital (HOMO and LUMO) and frontier orbital energy gap helping to exemplify the reactivity and kinetic stability of molecules are important parameters in the electronic studies [58,59]. The analysis of the wave function indicates that the electron absorption corresponding to the transition from the ground state to the first excited state is mainly defined by one electron excitation from the highest occupied orbital (HOMO) to the lowest unoccupied orbital (LUMO) [60].

The calculated HOMO-LUMO energy gap of the BFPT molecule is 3.9955eV. Meanwhile, the lowering of the energy gap describes that chemical activity and the eventual charge transfer takes place within the molecule, which influences the biological activity of the molecule. The positive phase is represented in red colour and the negative phase is represented in green colour. The HOMO-LUMO plot of BFPT molecule is given in Fig.6 and their orbital values are shown in Table 2.

As seen from the Fig. 6, the HOMO is located on the phenyl ring and bromine atom. The LUMO is located on entire molecule. Associated within the framework of molecular orbital theory, the ionization energy and electron affinity can be expressed by HOMO and LUMO orbital energies as $I = -E_{HOMO}$ and $A = -E_{LUMO}$. The global hardness, $\eta = 1/2(E_{LUMO} - E_{HOMO})$. The electron affinity can be used in combination

with ionization energy to give electronic chemical potential, $\mu = 1/2(E_{LUMO} + E_{HOMO})$. The global electrophilicity index, $\Psi = \mu^2 / 2\eta$ [61,62]. These parameters have been calculated and tabulated in Table 3. The value of $\eta$ of the BFPT molecule is 1.9977eV. Hence we concluded that the title compound belongs to hard material and have higher stability.

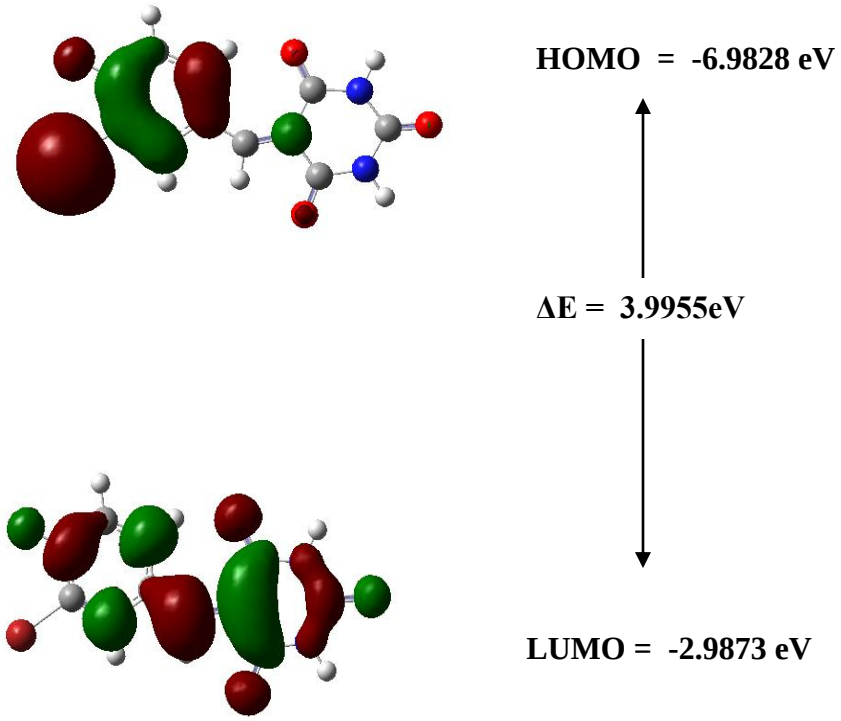


**Figure 6.** The frontier molecular orbitals of BFPT

DOS spectrum represents the number of energy level on the energy axis that the section has width dE and the spectrum is convoluted with Gaussian curves of heights equal to the calculated contributions for each orbital. The most important application of the DOS plot is to demonstrate MO (Molecular orbital) compositions and their contribution to chemical bonding [63]. DOS spectrum of BFPT is shown in Fig. S1.

*3.6 Electronic absorption spectra analysis*

Electronic transitions are usually classified according to the orbitals engaged or to specific parts of the molecule involved. Common types of electronic transition in organic compounds are π-π*, n-π*[64]. In order to understand the electronic transitions of BFPT, theoretical calculations on electronic absorption spectrum, capable of describing the spectra features of the molecule, were performed by TD-

DFT method. The theoretical calculation of UV spectral analysis of BFPT have been investigated in gas phase and the calculated excitation energies, oscillator strength (f) and wavelength (λ) and spectral assignment are given in Table S3.

**Table 2. The Frontier molecular orbital of BFPT**

| Orbitals | Orbital energies (a.u) | Orbital energies (eV) |
|---|---|---|
| $O_{73}$ | -0.3039 | -8.2699 |
| $O_{74}$ | -0.3002 | -8.1711 |
| $O_{75}$ | -0.2732 | -7.4361 |
| $O_{76}$ | -0.2719 | -7.4002 |
| $O_{77}$ | -0.2566 | -6.9828 |
| $V_{78}$ | -0.1097 | -2.9873 |
| $V_{79}$ | -0.0383 | -1.0446 |
| $V_{80}$ | -0.0190 | -0.5189 |
| $V_{81}$ | -0.0153 | -0.4179 |
| $V_{82}$ | -0.0094 | -0.2563 |

*O-Occupied orbital; V-Virtual orbital*

**Table 3.** Global reactivity descriptors of BFPT

| **Global reactivity descriptors** | **Values** |
|---|---|
| HOMO | -6.9824 |
| LUMO | -2.9871 |
| HOMO–LUMO energy gap (ΔE) | -3.9953 |
| Global hardness ($\eta$) | 1.9976 |
| Global softness (s) | 0.5006 |
| Chemical potential (μ) | -4.9847 |
| global electrophilicity index (Ψ) | 6.2192 |

The theoretical absorption wavelengths are compared with experimental wavelengths are shown in Table S3. TD-DFT calculations predict three transitions in UV-Vis region. The transition at 3.4116 eV(363 nm) and at 3.6350eV (341 nm) with oscillator strength 0.1618 and strong transition at 4.0301eV (307 nm) with higher oscillator strength 0.5655 in gasphase. The band at 272 nm in experimental spectrum corresponding to the calculated wavenumber at 307 nm with red shift of 35 nm and are assigned for π-π* transition. The calculated and visible absorption maxima of the title molecule corresponded to

the electronic transition between frontier orbitals, such as transition from HOMO-2 to LUMO, HOMO to LUMO, HOMO to LUMO +1. The theoretical and experimental UV-Vis spectrum is shown in Fig.S2.

*3.7 Non–linear optics*

The first hyperpolarizability (β) of this molecular system and related properties (α, β, Δα) of the title compound were calculated using B3LYP/6-31G(d,p) level of theory, based on finite field approach. In the presence of an applied electric field, the energy of system is a function of the electric field. Polarizability and hyperpolarizability characterize the response of a system in an applied electric field [65]. They determine not only the strength of molecular interaction and collision process but also the non-linear optical properties (N.L.O) of the system [66,67]. First order hyperpolarizability is a third rank tensor that can be described by 3×3×3 matrix. The 27 components of the 3D matrix can be reduced to 10 components due to the Kleinman symmetry [68]. It can be given in the lower tetrahedral format. It is obvious that the lower part of the 3×3×3 matrixes is a tetrahedral. The components of β are defined as the coefficients in the Taylor series expansion of the energy in the external electric field. When the external electric field is weak and homogeneous, this expansion becomes:

$$E = E_0 - \mu_\alpha F_\alpha - 1/2\alpha_{\alpha\beta}F_\alpha F_\beta - 1/6\beta_{\alpha\beta\gamma}F_\alpha F_\beta F_\gamma \quad (2)$$

Where $E^0$ is the energy of the unperturbed molecules, $F_\alpha$ the field at the origin $\mu_\alpha$, $\alpha_{\alpha\beta}$, and $\beta_{\alpha\beta}{}^{\gamma}$ are the components of dipole moment, polarizability and the first hyperpolarizabilities respectively. The total static dipole moment (μ), The mean polarizability ($\alpha_0$), The anisotropy of polarizability (Δα) and mean first hyperpolarizability ($\beta_0$) using x,y,z components. They are defined as...

$$\mu = \sqrt{\left(\mu_x^2 + \mu_y^2 + \mu_z^2\right)} \quad (3)$$

$$\alpha = \frac{\alpha_{xx} + \alpha_{xy} + \alpha_{xz}}{3} \quad (4)$$

$$\beta_0 = \left(\beta_x^2 + \beta_y^2 + \beta_z^2\right)^{1/2} \quad \text{and} \quad (5)$$

$$\beta_x = \beta_{XXX} + \beta_{XYY} + \beta_{XZZ}$$

$$\beta_Y = \beta_{YYY} + \beta_{XXY} + \beta_{YYZ}$$

$$\beta_Z = \beta_{ZZZ} + \beta_{XXZ} + \beta_{YYZ}$$

In the present study, the calculated dipole moment (μ), polarizability (α) and first hyperpolarizability ($\beta_0$) of the BFPT compound are 1.2977 Debye, $3.6998 \times 10^{-30} esu$ and

$14.56 \times 10^{-30} esu$ respectively and the values are shown in Table 4. The $\beta_0$ value of the title compound is 39 times greater than that of urea. These results indicate that the BFPT molecule is a good candidate of NLO material. Urea is one of the Prototypical molecular used in the study of the NLO properties of molecular systems. Therefore it was used frequently as a threshold value for comparative purposes.

To understand this phenomenon in the context of molecular orbital theory, we examined the molecular HOMO and LUMO of the title compound. When we see the first hyperpolarizability value, there is an inverse relationship between the first hyperpolarizability and HOMO-LUMO gap, allowing the molecular orbital's to overlap to have a proper electronic communication conjugation, which is a marker of the intramolecular charge transfer from the electron donating group through π-conjugation system to the electron accepting group [69,70].

Table 4. The molecular electric dipole moments μ (Debye), Polarizability ($\alpha_0$) and Hyperpolarizability ($\beta_0$) values of BFPT

| Parameters | B3LYP/6-31G(d,p) |
|---|---|
| μ | 1.2977 Debye |
| α | 3.6998 x$10^{-30}$*esu* |
| *Hyperpolarizability* ( $\beta_0$ ) | x$10^{-30}$*esu* |
| $\beta_{xxx}$ | -1140.35 |
| $\beta_{xxy}$ | 482.60 |
| $\beta_{xyy}$ | -227.36 |
| $\beta_{yyy}$ | 94.56 |
| $\beta_{xxz}$ | -283.46 |
| $\beta_{xyz}$ | 190.48 |
| $\beta_{yyz}$ | -59.86 |
| $\beta_{xzz}$ | -195.69 |
| $\beta_{yzz}$ | 1.46 |
| $\beta_{zzz}$ | 92.10 |
| $\beta_0$ | 14.56 x$10^{-30}$*esu* |

*Standard value for urea (**μ**=1.3732 Debye, $\beta_0$=0.3728x$10^{-30}$esu): **esu**-electrostatic unit

*3.8 NBO analysis*

NBO analysis provides the most accurate possible 'natural Lewis structure' because all orbital details are mathematically chosen to include the highest possible percentage of the electron density. A useful aspect of the NBO method is that it gives information about interactions in both filled and virtual orbital spaces that could enhance the analysis of intra-and intermolecular interactions. The second order Fock matrix was carried out to evaluate the donor-acceptor interactions in the NBO analysis [71]. The interactions result is a loss of occupancy from the localized NBO of the idealized Lewis structure into an empty non-Lewis orbital. For each donor (i) and acceptor (j), the stabilization energy $E^{(2)}$ associated with the delocalization $i \rightarrow j$ is estimated as

$$E^{(2)}=\Delta E_{ij}=q_i\frac{F(i,j)^2}{\varepsilon_j-\varepsilon_i} \qquad (7)$$

where $q_i$ is the donor orbital occupancy, are $\varepsilon_i$ and $\varepsilon_j$ diagonal elements and F(i, j) is the off diagonal NBO Fock matrix element. Natural bond orbital analysis provides an efficient method for studying intra and intermolecular bonding and interaction among bonds, and also provides a convenient basis for investigating charge transfer or conjugative interaction in molecular systems. Some electron donor orbital, acceptor orbital and the interacting stabilization energy resulted from the second-order micro-disturbance theory are reported [72]. The larger the $E^{(2)}$ value, the more intensive is the interaction between electron donors and electron acceptors, i.e. the more donating tendency from electron donors to electron acceptors and the greater the extent of conjugation of the whole system. Delocalization of electron density between occupied Lewis-type (bond or lone pair) NBO orbitals and formally unoccupied (anti-bond or Rydgberg) non-Lewis NBO orbitals correspond to a stabilizing donor–acceptor interaction. NBO analysis has beenperformed on the molecule at the DFT/B3LYP/6-31G(d,p) level of theory in order to elucidate the intramolecular, re-hybridization and delocalization of electron density within the molecule are shown in Table 5.

In the present study, the electron densities of the σ bonds are higher than π bonds. The lowering of the electron densities is due to transfer of lone pair electron from donor to acceptor (anti-bonding) orbital. This is evident from the table that the electron densities of σ N–C, N–H, C–C, C–H and C–X are higher in the range of 1.968-1.995 and their corresponding anti bonding orbital have weaker electron densities with lesser hyper conjugative energy. On the other hand, the occupancy of π $C_5$–$C_{11}$, $C_{14}$–$C_{16}$, $C_{15}$–$C_{17}$, $C_{19}$–$C_{21}$ decreased by increasing electron densities of their corresponding anti-bonding orbitals with maximum stabilization energy.

**Table 5.** Second order perturbation theory analysis of Fock matrix in NBO basis of BFPT

| Type | Donor (i) | ED/e | Acceptor (j) | ED/ e | [a]$E^{(2)}$ kJ/mol | [b]F(i,j) (a.u) | [c]E(j)-E(i) (a.u) |
|---|---|---|---|---|---|---|---|
| σ–σ* | $N_1$–$H_7$ | 1.9812 | $C_2$–$N_3$ | 0.0855 | 17.91 | 1.09 | 0.062 |
| | | | $C_5$–$C_6$ | 0.0728 | 15.44 | 1.08 | 0.057 |
| π–π* | $C_2$–$O_8$ | 1.9845 | $C_2$–$O_8$ | 0.3251 | 7.03 | 0.38 | 0.024 |
| σ–σ* | $N_3$–$C_4$ | 1.9885 | $C_2$–$O_8$ | 0.0102 | 10.84 | 1.43 | 0.054 |
| | | | $C_5$–$C_{11}$ | 0.0164 | 8.12 | 1.44 | 0.047 |
| π–π* | $C_4$–$O_{10}$ | 1.9778 | $C_5$–$C_{11}$ | 0.1744 | 17.24 | 0.4 | 0.038 |
| π–π* | $C_5$–$C_{11}$ | 1.7726 | $C_4$–$O_{10}$ | 0.2942 | 103.64 | 0.28 | 0.075 |
| | | | $C_5$–$C_{11}$ | 0.1744 | 8.41 | 0.3 | 0.022 |
| | | | $C_6$–$O_{12}$ | 0.2852 | 101.59 | 0.28 | 0.075 |
| | | | $C_{14}$–$C_{16}$ | 0.3990 | 38.62 | 0.29 | 0.048 |
| π–π* | $C_6$–$O_{12}$ | 1.9838 | $C_5$–$C_{11}$ | 0.1744 | 11.72 | 0.4 | 0.031 |
| σ–σ* | $C_{11}$–$H_{13}$ | 1.9689 | $C_4$–$C_5$ | 0.0677 | 34.73 | 0.95 | 0.08 |
| | | | $C_5$–$C_{11}$ | 0.0164 | 5.36 | 1.13 | 0.034 |
| | | | $C_{14}$–$C_{15}$ | 0.0251 | 23.97 | 1.06 | 0.07 |
| π -π* | $C_{14}$–$C_{16}$ | 1.5995 | $C_5$ –$C_{11}$ | 0.1744 | 98.07 | 0.28 | 0.077 |
| | | | $C_{15}$–$C_{17}$ | 0.2779 | 84.56 | 0.28 | 0.07 |
| | | | $C_{19}$–$C_{21}$ | 0.4318 | 78.87 | 0.25 | 0.062 |
| π–π* | $C_{15}$–$C_{17}$ | 1.6630 | $C_{14}$–$C_{16}$ | 0.3990 | 69.91 | 0.27 | 0.061 |
| | | | $C_{19}$–$C_{21}$ | 0.4318 | 115.56 | 0.25 | 0.076 |
| n–π* | $N_1$ | 1.6568 | $C_2$–$O_8$ | 0.3251 | 244.05 | 0.28 | 0.114 |
| | | | $C_6$–$O_{12}$ | 0.2852 | 229.37 | 0.28 | 0.112 |
| n–π* | $N_3$ | 1.6576 | $C_2$–$O_8$ | 0.3251 | 241.67 | 0.28 | 0.114 |
| | | | $C_4$–$O_{10}$ | 0.2942 | 231.42 | 0.27 | 0.111 |
| n–σ* | $O_8$ | 1.8436 | $N_1$–$C_2$ | 0.0845 | 113.97 | 0.67 | 0.123 |
| | | | $C_2$–$N_3$ | 0.0855 | 114.64 | 0.67 | 0.123 |
| n–σ* | $O_{10}$ | 1.8642 | $N_3$–$C_4$ | 0.0788 | 112.09 | 0.68 | 0.122 |
| | | | $C_4$–$C_5$ | 0.0677 | 74.73 | 0.7 | 0.101 |
| | | | $C_{15}$–$H_{18}$ | 0.0272 | 19.41 | 0.79 | 0.055 |
| n–σ* | $O_{12}$ | 1.8556 | $N_1$–$C_6$ | 0.0789 | 112.59 | 0.68 | 0.123 |
| | | | $C_5$–$C_6$ | 0.0728 | 83.89 | 0.66 | 0.105 |
| | | | $C_{11}$–$H_{13}$ | 0.0210 | 8.16 | 0.72 | 0.034 |
| n–π* | $Br_{23}$ | 1.9348 | $C_{19}$–$C_{21}$ | 0.4318 | 42.59 | 0.28 | 0.053 |
| n–π* | $F_{24}$ | 1.9013 | $C_{19}$–$C_{21}$ | 0.4318 | 97.74 | 0.41 | 0.095 |
| π*–π* | $C_4$–$O_{10}$ | 0.2942 | $C_5$–$C_{11}$ | 0.1744 | 285.73 | 0.02 | 0.076 |
| π*–π* | $C_6$ –$O_{12}$ | 0.2852 | $C_5$–$C_{11}$ | 0.1744 | 297.78 | 0.02 | 0.068 |
| π*–π* | $C_{14}$–$C_{16}$ | 0.3990 | $C_5$–$C_{11}$ | 0.1744 | 685.55 | 0.01 | 0.07 |
| | | | $C_{15}$–$C_{17}$ | 0.2779 | 805.8 | 0.01 | 0.08 |
| π*–π* | $C_{19}$–$C_{21}$ | 0.4318 | $C_{14}$–$C_{16}$ | 0.3990 | 673.46 | 0.02 | 0.08 |
| | | | $C_{15}$–$C_{17}$ | 0.2779 | 366.73 | 0.04 | 0.083 |

[a] E(2) means energy of hyper conjugative interaction (stabilization energy).
[b] F(i,j) is the fork matrix element between i and j NBO orbitals.
[c] Energy difference between donor(i) and acceptor(j) NBO orbitals.

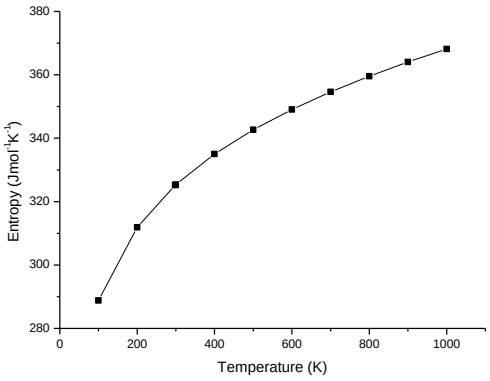


**Figure 7.** Correlation graph between Temperature Vs Entropy of BFPT

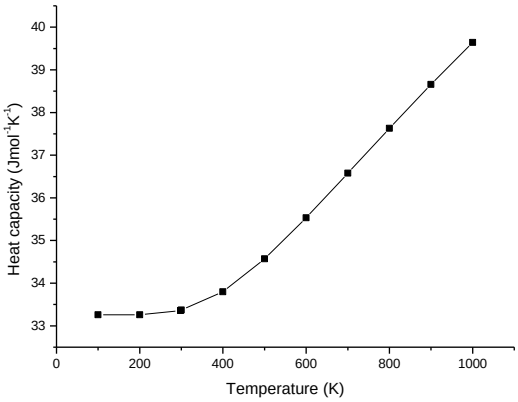


**Figure 8.** Correlation graph between Temperature Vs Heat capacity of BFPT

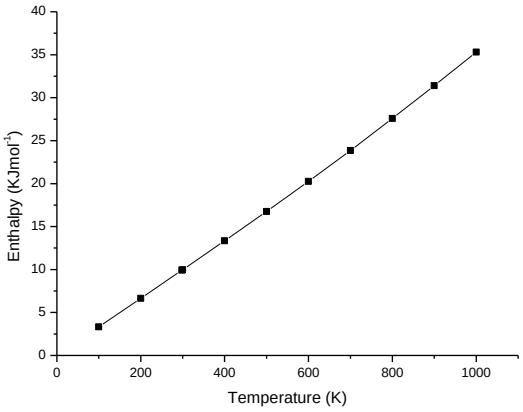


**Figure 9.** Correlation graph between Temperature Vs Enthalpy of BFPT

The hyper conjugative interactions are observed in benzene and pyrimidine ring for donor and acceptor orbitals of $\pi(C_{14}–C_{16})\rightarrow \pi^*(C_5–C_{11}, C_{15}–C_{17}, C_{19}–C_{21})$, $\pi(C_{15}–C_{17})\rightarrow\pi^*(C_{14}–C_{16}, C_{19}–C_{21})$,

$\pi(C_{19}–C_{21})\rightarrow\pi^*(C_{14}–C_{19})$ and $\pi(C_5–C_{11})\rightarrow\pi^*(C_4–O_{10}$, $C_6–O_{12}$, $C_{14}–C_{16})$ are shows maximum hyperconjugative energy, in which pyrimidine ring have higher stabilization energy. The π–π* interaction of BFPT molecule reveals that intra molecular charge transfer occur in pyrimidine ring with maximum stabilization energy.

It is evident from the table, the n–π* interaction for LPN1$\rightarrow\pi^*(C_2–O_8$, $C_6–O_{12})$, LPN3$\rightarrow\pi^*(C_2–O_8$, $C_4–O_{10})$ have higher hyperconjugative energy leading stabilization of 244.05 & 229. 37 and 241.67 & 231.42 KJ/mol respectively, during the n– π* interaction more energy delocalization takes place. The n–$\sigma^*$ transitions for $O_8$, $O_{10}$, $O_{12}$, $Br_{23}$ and $F_{24}$ have lesser stabilization energy then n–π* interaction.

**Table 6.** Thermodynamic parameters of BFPT

| T (K) | S(J/mol.K) | Cp(J/mol.K) | ddH (kJ/mol) |
|---|---|---|---|
| 100.00 | 288.84 | 33.26 | 3.33 |
| 200.00 | 311.89 | 33.26 | 6.65 |
| 298.15 | 325.18 | 33.36 | 9.92 |
| 300.00 | 325.39 | 33.37 | 9.98 |
| 400.00 | 335.04 | 33.80 | 13.34 |
| 500.00 | 342.66 | 34.57 | 16.75 |
| 600.00 | 349.05 | 35.53 | 20.26 |
| 700.00 | 354.60 | 36.58 | 23.86 |
| 800.00 | 359.56 | 37.63 | 27.57 |
| 900.00 | 364.05 | 38.66 | 31.39 |
| 1000.00 | 368.17 | 39.64 | 35.30 |

*3.9 Thermodynamic properties*

The total energy of a molecule is the sum of translational, rotational, vibrational and electronic energies, i.e., $E = E_t + E_r + E_v + E_e$. The statistical thermo chemical analysis of BFPT is carried out considering the molecule to be at room temperature of 298.15 K and one atmospheric pressure.

The thermodynamic parameters, like rotational constant, zero point vibrational energy (ZPVE) of the molecule by DFT method with B3LYP are presented in Table S4. On the basis of vibrational analysis and statistical thermodynamics, the standard thermodynamic functions: heat capacity (Cp), entropy (S), and enthalpy (ΔH) were obtained and listed in Table 6.

As is evident from Table 7, all the values of Cp, S, and ΔH increases with the increase of temperature from 100K to1000K, which is attributed to the enhancement of the molecular vibration while the temperature increases because at a constant pressure (db = 1 atm) values of Cp, S, and ΔH are equal to the quantity of temperature [73]. The correlations between these thermodynamic properties and temperatures T are shown in Fig. 7-9.

## 4. CONCLUSION

The calculated vibrational frequencies obtained by DFT calculations are in good agreement with the experimental values obtained for the investigated molecule. The energies of important molecular orbital's absorption wavelength ($\lambda_{max}$), oscillator strength and excitation energies of the compound were also determined from TD-DFT method and compared with experimental values. The FMO analysis of BFPT molecule explains eventual charge transfer interaction taking place within the molecule. The MEP map shows that the negative potential sites are on the electronegative atoms while the positive potential sites are around the hydrogen atom. The predicted NLO properties of the title compound much greater than urea. Therefore the compound is a good candidate as a second order non-linear optical material. The thermodynamic properties of the title compound at different temperatures have been calculated. It is seen that the heat capacities, entropies and enthalpies increase with the increasing temperature owing to the intensities of the molecular vibrations increase with increasing temperature.

## References


[1] Wurthner, F.; Yao, S.; Heise, B.; Tshierske, C.; "Hydrogen bond directed formation of liquid-crystalline merocyanine dye assemblies", *Chem. Comun.* **2001**, 21, 2260-2261.

[2] Rezende, M.C.; Campodonico, P; Abuin, E.; "Merocyanine-type dyes from barbituric acid derivatives", *Spectrochim. Acta. partA*, **2001**, 57(6), 1183-1190.

[3] Archana, S.; Srivastava, V.K.; Kumar, A.; "Synthesis and Anticonvulsant Activity of 1-Acetyl-5-arylidenyl-3-(2'-oxo/thio-barbiturinyl)-2-pyrazolines", *Arzneim.-Forsch*., **2002**, 52(11), 787-791.

[4] Goel, B.; Sharma, S.; Bajaj, K.; Bansal, D.; Singh, T.; Malik, N.; Lata, S.; Tyagi, C.; Panwar, H.; Agarwal, A.; Kumar, A.; 'Synthesis and CNS depressant of newer spirobarbiturates", *Ind. J. Pharm. Sci*. **2005**, 67, 194-199.

[5] Osman, A. N.; Kandeel, M. M.; Said M. M,; Ahmed, M.; "Synthesis and Anticonvulsant activity of some spiro compounds derived from barbituric and Thiobarbituric acids", *Indian J. Chem., Sect B*, **1996**, 35B, 1073-1078.

[6] Archana, A.; Rani. P; Bajaj, K.; Srivastava, V.K.; Chandra, R.; Kumar, A; "Synthesis of newer Indolyl/Phenothiazinyl substituted 2-oxo/Thiobarbituric acid derivatives as potent anticonvulsant agents", *Arzneim.-Forsch*., **2003**, 53, 301-306.

[7] Sarma, G.V.S.R.; Rao, J.V.; Suresh, B.; "Synthesis and pharmacological evaluation of 1-[2,6,8-trisubstituted-4(3H)-oxoquinazolin-3-yl]-3-(4-substitutedphenyl) thiobarbiturates", *Ind. J. Pharma. Sci*. **1999**, 61(2), 105-109.

[8] Gupta, K.P.; Gupta, R.C.; Bhargava, K.P.; Ali, B.; "Inhibition of brain respiration by new anticonvulsant benzylidenethiobarbiturates", *Eur. J. Med.Chem*. **1982**, 17, 448-452.

[9] Rastogi, V.K.; Mittal, H.P.; Sharma, Y.C.; Sharma, S.N.; "*Spectroscopy of Biological Molecules*", Royal Soc. Chem., London, **1991**.

[10] Hester, R.E.; Girling, R.B.; "*Spectroscopy of Biological Molecules*", Royal Society of Chemistry, London, UK, **1991**.

[11] Bandekar, J.; Zundel, G.; "Normal coordinate analysis treatment on uracil in solid state", *Spectrochim. Acta part A*,**1983**, 39(4), 343–355.

[12] Kwan, P.; Brodie, M.J.; "Phenobarbital for the treatment of epilepsy in the 21st century: A critical review", *Epilepsia*. **2004**, 45(9), 1141–1149.

[13] Aruna, S.; Shanmugam, G.; "Vibrational assignments of six-membered heterocyclic compounds: Normal vibrations of 6-aminouracil and 6-amino2-thiouracil", *Spectrochim. Acta partA.* **1985**, 41, 531–536.

[14] Portalone, G.; Ballirano, P.; Maras, A.; "The crystal structure of 3-methyluracil from X-ray powder diffraction data", *J. Mol. Struct*., **2002**, 608, 35–39.

[15] Grosmaire, L.; Delabre,J.L.; "Vibrational spectra of 6-methyluracil, 6-methyl-2-thiouracil and their deuterated analogues", *J. Mol. Struct*. **2012**, 1011, 42–49.

[16] Yaniv, M.; Folk, W.R.; "The nucleotide sequences of the two glutamine transfer ribonucleic acids from Escherichia coli", *J. Bio. Chem*. **1975**, 250, 3243–3253.

[17] Cirak, C.; Sert, Y.; Ucun, F.; "Experimental and computational study on molecular structure and vibrational analysis of a modified biomolecule: 5-Bromo-2′-deoxyuridine", *Spectrochim. Acta partA*. **2012**, 92, 406–414.

[18] Demi rbas, N.; Ugurluoglu, R.; Demirbaş, A.; "Synthesis of 3-alkyl(aryl)-4-alkylidenamino-4,5-dihydro-1H-1,2,4-triazol-5-ones and 3-alkyl-4-alkylamino-4,5-dihydro-1H-1,2,4-triazol-5-ones as antitumor agents*", Bioorg. Med. Chem*. **2002**, 10, 3717–3723.

[19] Elinson, M.N.; Vereshchagin, A.N.; Stepanov,N.O.; Zaimovskaya, T.A.; Merkulova,V.M.; Nikishin,G.I.; "The first example of the cascade assembly of a spirocyclopropane structure: direct transformation of benzylidenemalononitriles and N,N′-dialkylbarbituric acids into substituted 2-aryl-4,6,8-trioxo-5,7-diazaspiro[2.5]octane-1,1-dicarbonitriles", *Tetrahedron Lett*. **2010**, 51, 428–431.

[20] Amir, M.; Javed, S.A.; Kumar, H.; "Pyrimidine as anti-inflammatory agent: A review", *Ind. J. Pharm. Sci*. **2007**, 69, 337–343.

[21] Barakat, A.; Al–Majid, A.M.; Al–Najjar, H.J.; "Mabkhot,Y.N.; Javaid, S.; Yusuf, S.; Choudhary, M.I.; Zwitterionic pyrimidinium adducts as antioxidants with therapeutic potential as nitric oxide scavenger", *Eur. J. Med. Chem*. **2014**, 84, 146–154.

[22] Ray, R.; Krishna, S.H.; Sharma, J.D.; Limaye, S.N.; "Variations in the physico-chemical parameters of some 5a and 5b substituted barbiturate derivatives", *Asian J. Chem.* **2007**, 19, 2497–2501.

[23] Brunton, L.L.; Lazo, J.S.; Lazo, P.; Keith, L.; Goodman & Gilman's "*The Pharmacological Basis of Therapeutics*", McGraw–Hill: New York, NY, USA, **2006**.

[24] Fillaut, J.L.; de Los Rios, I.; Masi, D.; Romerosa, A.; Zanobini, F.; Peruzzini, M.; "Synthesis and Structural Characterization of (Carbene)ruthenium Complexes Binding Nucleobases", *Eur. J. Inorg. Chem*. **2002**, 2002, 935–942.

[25] Temiz–Arpaci, O.; Ozdemir, A.; Yalcin, I.; Yildiz, I.; Aki–Sener, E.; Altanlar, N.; Synthesis and antimicrobial activity of some 5-[2-(morpholin-4-yl)acetamido] and/or 5-[2-(4-substituted piperazin-1-yl)acetamido]-2-(p-substituted phenyl)benzoxazoles, *Arch.Pharm*, **2005**, 338, 105–111.

[26] Arzamastsev, A.P.; Luttseva,T.Y.; Sadchikova,N. P.; "Methods for the Analysis and Standardization of Drugs Belonging to the Class of Barbituric Acid Derivatives", *Pharm. Chem. J*. **2001**, 35, 453-457.

[27] Roux, M.V.; Temprado, M.; Notario, R.; EmelYanenko, V.N.; Verevkin, S.P.; Structure-energy relationship in barbituric acid: A calorimetric, computational, and crystallographic study, *J. Phys. Chem*. **2008**, 112, 7455-7465.

[28] Jamroz, M.H.; "*Vibrational Energy Distribution Analysis*": VEDA4 program, Warsaw, Poland, **2004**.

[29] Erdogdu, Y.; Unsalan, O.; Gulluoglu, M.T.; "FT-Raman, FT-IR spectral and DFT studies on 6, 8-dichloroflavone and 6, 8-dibromoflavone", *J. Raman Spectrosc*. **2010**, 41, 820-828.

[30] Erdogdu, Y.; Unsalan, O.; Amalanathan, M.; Hubert, J. I.; "Infrared and Raman spectra, vibrational assignment, NBO analysis and DFT calculations of 6-aminoflavone", *J. Mol. Struct.* **2010**, 980, 24-30.

[31] Babykala, R.; Kalaivani, D.; N,N-Diethylanilinium 5-(5-chloro-2,4-dinitrophenyl)-2,6-dioxo-1,2,3,6-tetrahydropyrimidin-4-olate, *Acta. Cryst*. **2013**, E69, 0398–0399.

[32] Singh, J.S.; "FT-IR and Raman spectra, ab initio and density functional computations of the vibrational spectra, molecular geometries and atomic charges of uracil and 5-halogenated uracils (5-X-uracils; X = F, Cl, Br, I)", *Spectrochim. Acta Part A*. **2014**, 117, 502–518.

[33] Chandra, S.; Saleem, H.; Sundraganesan, N.; "Experimental and theoretical vibrational spectroscopic and HOMO, LUMO studies of 1,3-dimethylbarbituric acid", *Ind. J. Chem*. **2009**, 48A, 1219–1227.

[34] Kalaichelvan, S.; Dominic Joshua, B.; Sundaraganesan, N.; "FT-IR, FT-Raman spectra and ab initio HF and DFT calculations of 2-nitro- and 4-nitrobenzaldehydes", *Ind. J. Chem*. **2008**, 47A, 1632–1641.

[35] Jag, M.; "*Organic Spectroscopy–Principles and Applications*", Second ed., Narosa Publishing House, New Delhi, **2001**.

[36] Sharma, Y.R.; "*Elementary Organic Spectroscopy Principles and Chemical Applications*", S. Chand & Company, Ltd., New Delhi, **1994**, 92–93.

[37] Jamroz, M. H.; CzDobrowolski, J.; Brzozowksi, R.; "Vibrational modes of 2,6-, 2,7-, and 2,3-diisopropylnaphthalene-A DFT study", *J. Mol. Struct*. **2006**, 787, 172-183.

[38] Silver stein, Clayton, Bessseler, "*Spectroscopic Identification of organic compounds*", Wiley, Newyork, **1976**.

[39] Barbara H. Stuart, "*Infrared spectroscopy: Fundamentals and Applications, University of Technology*", Sydney, Australia.

[40] Bellamy, L.J.; "*The Infrared Spectra of Complex Molecules*", third ed., Wiley, Newyork, **1975**.

[41] Varsanyi, G.; "*Assignments for Vibrational Spectra of Seven hundred Benzene Derivatives*", AdamHilger, London, **1974.**

[42] Alcerreca, G.; Sanabria, R.; Miranda, R.; Arroyo, G.; Tamariz, J.; Delgado, F.; "Preparation of Benzylidene Barbituric Acids Promoted by Infrared Irradiation in Absence of Solvent", *synth. commun*, **2000**, 30(7), 1295–1301.

[43] Roeges, N.P.G.; "*A Guide to the Complete Interpretation of Infrared Spectra of Organic Structure*", Wiley, New York, **1994**.

[44] Barthes, M.; De Nunzio, G.; Ribet, M.; "Polarons or proton transfer in chains of peptide groups", *Synth. Met*. **1996**, 76, 337–340.

[45] Shinde, V.S.; Jadhav, W. N.; Karade, N.N.; "Three component solvent-free synthesis and fungicidal activity of substituted pyrimido[4,5-d]pyrimidine-2-(1H)-one", *Oriental J. Chem*. **2010**, 26(1), 307–317.

[46] Sert, Y.; Abdulghafoor, A.; Al–Turkistani,; "Experimental FT-IR, laser-Raman and DFT spectroscopic analysis of a potential chemotherapeutic agent 6-(2-methylpropyl)-4-oxo-2-sulfanylidene-1,2,3,4-tetrahydropyrimidine-5-carbonitrile", *Spectrochim. Acta Part A*. **2014**, 120, 97–105.

[47] Anbarasan, R.; Dhandapani, A.; Manivarman, S.; Subashchandrabose, S.; Saleem, H.; "Synthesis and spectroscopical study of Rhodanine derivative using DFT approaches", *Spectrochim. Acta partA*. **2015**, 146, 261–272.

[48] Janaki, A.; Balachandran, V.; Lakshmi, A.; "First order molecular hyperpolarizabilities and intramolecular charge transfer from vibrational spectra of NLO material 2,6-dichloro-4-nitroaniline", *Ind. J. Pure & Applied Phys*. **2013**, 51, 601-614.

[49] Bellamy, L.J.; "*The Infrared Spectra of Complex Molecules*", Chapman and Hall, London, **1980**.

[50] Balachandran, V.; Santhi, G.; "Vibrational spectra, NBO, HOMO-LUMO and NMR (1H and 13C) analyses of 5-bromo-2-methoxybenzaldehyde", *Elixir. Vib. Spec*. **2012**, 52, 11425–11436.

[51] Sylvestre, S.; Sebastian, S.; Edwin, S.; "Vibrational spectra (FT-IR and FT-Raman), molecular structure, natural bond orbital, and TD-DFT analysis of L-Asparagine monohydrate by density functional theory approach", *Spectrochim. Acta PartA*, **2014**, 133, 190–200.

[52] Murray, J.S.; Sen, K.; "*Molecular electrostatic potentials, Concepts and Applications*", Elsevier, Amsterdam, **1996**.

[53] Scrocco, E.; Tomasi, J.; Lowdin (Ed), "*Advances in quantum chemistry*", Academic press, New York, **1978**.

[54] Okulik, N.; Jutert, A.H.; "Theoretical analysis of the reactive sites of non–steroidal anti–inflammatory drugs", *Int. J. Mol. Des*, **2005**, 4, 17–30.

[55] Sidir, I.; Sidir, Y.G.; Kumalar, M.; Tasa, E.; "Ab initio Hartree–Fock and density functional theory investigations on the conformational stability, molecular structure and vibrational spectra of 7-acetoxy-6-(2,3-dibromopropyl)-4,8-dimethylcoumarin molecule", *J. Mol. Struct*, **2010**, 964, 134-151.

[56] Kavitha, E.; Sundaraganesan, N.; Sebastian, S.; Kurt, M.; "Molecular structure, anharmonic vibrational frequencies and NBO analysis of naphthalene acetic acid by density functional theory calculations", *Spectrochim. Acta part A*, **2010**, 77(3), 612–619.

[57] Chaitanya, K.; "Molecular structure, vibrational spectroscopic (FT-IR, FT-Raman), UV–vis spectra, first order hyperpolarizability, NBO analysis, HOMO and LUMO analysis, thermodynamic properties of benzophenone2,4-dicarboxylic acid by ab initio HF and density functional method", *Spectrochim. Acta part A*, **2012**, 86, 159–173.

[58] Kavitha, E.; Sundaraganesan, N.; Sebastian, S.; "Molecular structure, vibrational spectroscopic and HOMO, LUMO studies of 4-nitroaniline by density functional method", *Ind. J. Pure Appl. Phys*. **2010**, 48, 20–30.

[59] Jayaprakash, A.; Arjunan, V.; Mohan, S.; "Vibrational spectroscopic, electronic and quantum chemical investigations on 2,3-hexadiene", *Spectrochim. Acta partA*, **2011**, 81, 620–630.

[60] Subashchandrabose, S.; Saleem, H.; Erdogdu, Y.; Rajarajan, G.; Thanikachalam, V.; "FT-Raman, FT-IR spectra and total energy distribution of 3-pentyl-2,6-diphenylpiperidin-4-one: DFT method", *Spectrochim. Acta part A*, **2011**, 82, 260–269.

[61] Vijayakumar, T.; Hubert Joe, I.; Nair, C.P.R.; Jayakumar, V.S.; "Efficient π electrons delocalization in prospective push–pull non-linear optical chromophore 4-[N,N-dimethylamino]-4′-nitro stilbene (DANS): A vibrational spectroscopic study", *Chem. Phys.* **2008**, 343(1), 83–99.

[62] Govindarajan, M.; Karabacak, M.; Suvitha, A.; Periandy, S.; "FT-IR, FT-Raman and UV spectral investigation: Computed frequency estimation analysis and electronic structure calculations on chlorobenzene using HF and DFT", *Spectrochim. Acta part A*, **2012**, 88, 37–48.

[63] O'Boyle, N.M, "*Surface Studies and Density Functional Theory Analysis of Ruthenium Polypyridyl Complexes*", Dublin City University, **2004**.

[64] Zhang, R.; Dub, B.; Sun, G.; Sun, Y.; "Experimental and theoretical studies on o-, m- and p-chlorobenzylidene aminoantipyrines", *Spectrochim. Acta part A*, **2010**, 75A, 1115–1124.

[65] Zhang, C.R.; Chen, H.S.; Wang, G.H.; "Structure and Properties of Semiconductor Microclusters GanPn(n=1-4):A First Principle Study", *Chem. Res. Chinese U*. **2004**, 20, 640– 643.

[66] James, C.; Amal Raj, A.; Raghunathan, R.; Hubert Joe, I.; Jayakumar, V.S.; "Structural conformation and vibrational spectroscopic studies of 2,6-bis(p-N,N-dimethylbenzylidene)cyclohexanone using density functional theory", *J. Raman Spectrosc.* **2006**, 379(12), 1381–1392.

[67] Liu, J.N.; Chen, Z.R.; Yuan, S.F.; "Study on the prediction of visible absorption maxima of azobenzene compounds", *J. Zhejiang Univ*. B6, **2005**, 584–589.

[68] Colthup, N.B.; Daly, L.H.; Wiberley, S.E.; "*Introduction to Infrared and Raman Spectroscopy*", 3rd edition, MA: Academic press, Boston, **1990**.

[69] Ruiz Delgado, M.C.; Hernandez, V.; Casado, J.; Lopez Navarre, J.T.; Raimundo, J.M.; Blanchard, P.; Roncali, J.; "Vibrational study of push–pull chromophores for second-order non-linear optics derived from rigidified thiophene π-conjugating spacers", *J. Mol. Struct*, **2003**, 151, 651-653.

[70] Abraham, J.P.; Sajan, D.; Shettigar, V.; Dharmaprakash, S.M.; Nemec, I.; Joe, I.H.;Jayakumar, V.S.; "Efficient π-electron conjugated push–pull nonlinear optical chromophore 1-(4-methoxyphenyl)-3-(3,4-dimethoxyphenyl)-2-propen-1-one: A vibrational spectral study", *J. Mol. Struct*, **2009**, 917(1), 27-36.

[71] Szafran, M.; Komasa, A.; Adamska, E.B.; "Crystal and molecular structure of 4-carboxypiperidinium chloride (4-piperidinecarboxylic acid hydrochloride)", *J. Mol. Struct. (Theochem)*, **2007**, 827, 101-107.

[72] Jun–na, L.; Zhi–rang, C.; Shen–fang, Y.; "Study on the prediction of visible absorption maxima of azobenzene compounds", *J. Zhejiang Univ. Sci.6B*, **2005**, 584-590.

[73] Ott, J.B.; Boerio-Goates, J.; "*Calculations from Statistical Thermodynamics*", Academic Press, **2000**.

*The authors declare no conflict of interest*